PERGAMON

Polyhedron 18 (1999) 2869–2878

POLYHEDRON

www.elsevier.nl/locate/poly

Chemistry of azopyrimidines. Part II. Synthesis, spectra, electrochemistry and X-ray crystal structures of isomeric dichloro bis[2-(arylazo)pyrimidine] complexes of ruthenium(II)☆

Prasanta K. Santra[a], Tarun K. Misra[a], Debasis Das[a], Chittaranjan Sinha[a,*], Alexandra M.Z. Slawin[b], J. Derek Woollins[b]

[a]*Department of Chemistry, The University of Burdwan, Burdwan 713104, India*
[b]*Loughborough University, Loughborough, LE11 3TU, UK*

Received 23 March 1999; accepted 5 July 1999

Abstract

2-(Arylazo)pyrimidines (aapm, **3**) are new N,N′- chelating ligands in the azoimine family and were reacted with $RuCl_3$ in ethanol under refluxing conditions. Three isomers of the composition $Ru(aapm)_2Cl_2$ have been chromatographically separated and are established as having *trans–cis–cis* (tcc), *cis–trans–cis* (ctc) and *cis–cis–cis* (ccc) configurations with reference to the order of coordination pairs as Cl; N(pyrimidine), N and N(azo), N′. Two of the three isomeric structures have been confirmed by X-ray crystallography. In both of these structures, the Ru–N(azo) distances are relatively shorter than those of Ru–N(pyrimidine), indicating stronger bonding in the former and the presence of a Ru-(aapm) π-interaction that is localised in the Ru-azo fragment. The isomer configuration is supported by IR and ^1H NMR data. The complexes exhibit $t_2(Ru)\rightarrow\pi^*$(aapm) MLCT transitions in the visible region. Redox studies show the Ru(III)/Ru(II) couple in the green complexes [tcc-$Ru(aapm)_2Cl_2$] at 1.1–1.2 V and in the blue complexes [ctc- and ccc-$Ru(aapm)_2Cl_2$] at 1.2–1.4 V versus saturated calomel electrode (SCE) and two successive azo reductions. The difference in the first metal and ligand redox potentials is linearly correlated with ν_{CT} [$t_2(Ru)\rightarrow\pi^*$(aapm)].

Keywords: Azopyrimidines; High potential Ru(II) complexes; Isomers; Structures

1. Introduction

The π-acidity of the azoimine group, –N=N–C=N–, and its ability to stabilise the low valent metal redox state have encouraged us to study its chemistry and to design a molecular architecture with this function [1–32]. An imine group in a heterocyclic backbone with a pendant azo arm, i.e., arylazoheterocycles, have been extensively studied with respect to 2-(arylazo)pyridines (aap, **1**) [1–22]. The ruthenium complexes of these ligands are known in some detail [1–19]. Progress in the azoimine chemistry of azopyridines has encouraged us to explore the chemistry of this function in other heterocycles. Our first successful design was 2-(arylazo)imidazoles (**2**) [23–32].

To follow our interest in azoimine compounds with better π-acidity than that of aap (**1**), we synthesised a third member of the azoimine family, 2-(arylazo)pyrimidine (aapm, **3**). Pyrimidine was chosen because of its higher π-acidity than that found in conventional widely used pyridine bases [33–37] and also due to its biochemical importance [38–44]. Pyrimidine is an active component [38–44] of antibiotics, antimicrobials, anticonvulsants, antispasmatics, antineoplastics (e.g. bleomycin) and antidiabetogenics, and many derivatives have been used in seed dressings, crop-disease control and veterinary drugs etc. In coordination chemistry, the *meta*-related nitrogen in pyrimidine has played an important role for connecting different metals, transmitting antiferromagnetic interactions and for obtaining magnetic systems of high nuclearity [45–52]. Because of the peripheral N heteroatom, the excited state of the pyrimidine moiety undergoes protonation in aqueous solution and the complexes exhibit proton-dependent photophysics and photochemistry [53]. Recently, the design of molecular architecture with pyrimidine and bipyrimidine has aroused interest in the fields of coordination, bioinorganic and magnetochemistry [53–62]

☆For part I, see Polyhedron 18 (1999) 1909–1915.

*Corresponding author. Tel.: +91-0342-60810; fax: +91-0342-64452.
E-mail address: bdnuvlib@giascl01.vsnl.net.in (C. Sinha)

0277-5387/99/$ – see front matter
PII: S0277-5387(99)00189-8

on account of their interactions with metal ions. In this report, we describe the synthesis, spectral studies, redox properties and single crystal X-ray structures of ruthenium(II) complexes of 2-(arylazo)pyrimidines.

2. Experimental

2.1. Materials, general procedure and measurements

2-Aminopyrimidine was purchased from Aldrich. Ruthenium trichloride was digested three times with conc. HCl and evaporated to dryness before use, as described previously [31]. Nitrosoaromatics were prepared using known procedures [23–26]. The purification of acetonitrile and the preparation of tetrabutylammonium perchlorate (TBAP) for electrochemical work were carried out as before [31]. Dinitrogen was purified by bubbling it through an alkaline pyrogallol solution. All other chemicals and solvents were of reagent grade and were used without further purification. Commercially available alumina (neutral) and silica gel (SRL) were used for column chromatography. Spectroscopic data were obtained using the following instruments: UV–Vis spectra, Shimadzu UV160A; IR spectra (KBr disk, 4000–200 cm^{-1}), FTIR JASCO model 420; ^1H NMR spectra, Bruker (AC) 300 MHz FTNMR spectrometer. Electrochemical measurements were performed using computer-controlled PAR model 270 VERSASTAT Electrochemical instruments with Pt-bead and GC-electrodes. All measurements were carried out under a dinitrogen environment at 298 K with reference to saturated calomel electrode (SCE) in acetonitrile. The reported potentials are uncorrected for junction potential.

2.2. Preparation of ligands

2-(Arylazo)pyrimidines (**3**) were synthesised by condensing 2-aminopyrimidine with nitrosoaromatics. A representative case is detailed below. The available information on 2-(arylazo)pyridine [20,21] served as a guide for setting up experimental conditions.

2.3. 2-(Phenylazo)pyrimidine (papm, **3a**)

To a nitrogen-flushed solution of 2-aminopyrimidine (2.0 g, 0.021 mol) in dry benzene (30 cm^3) with sodium (1 g) was added nitrosobenzene (2.5 g, 0.023 mol) in small portions for 2 h under refluxing conditions. The reaction was continued for 3 h and cooled to room temperature. The dark red solution obtained was then filtered and the filtrate was washed with water (3×20 cm^3). It was then evaporated to reduce the volume to 5 cm and chromatographed on a silica gel (60–120 mesh) column (30×1 cm) prepared in pet-spirit (60–80°C). A light yellow band was eluted with pet-spirit and rejected. A red band was then eluted with benzene and collected. Evaporation of solvent gave a gummy mass of the ligand. The yield was 1.2 g (31%).

2-(*p*-Tollylazo)pyrimidine [*p*-tapm (**3b**)] (28%, gummy) and 2-(*p*-chlorophenylazo)pyrimidine (*p*-clpapm, **3c**) (40%, semi solid) were prepared similarly.

2.4. Preparation of complexes tcc- and ctc-dichlorobis[2-(phenylazo)pyrimidine]ruthenium(II), $Ru(papm)_2Cl_2$ (green tcc, **4a**; blue ctc, **4b**)

Nitrogen gas was bubbled through a brown solution of $RuCl_3 \cdot 3H_2O$ (0.13 g, 0.5 mmol) in 20 cm^3 of ethanol. Then, 0.22 g (1.2 mmol) of papm in 5 cm^3 of ethanol was added. The mixture was refluxed under nitrogen, with magnetic stirring, for 10 h. During this period, the solution turned green, then bluish green with a dark precipitate. The solution was cooled to room temperature, filtered, and the solid was washed thoroughly with water, ethanol and finally with Et_2O. It was then dried in a vacuum desiccator over P_4O_{10}. The dried product was dissolved in a small volume of CH_2Cl_2 and was chromatographed on an alumina (neutral) column (30×1 cm). A blue band was eluted using 9:1(v/v) benzene–acetonitrile. Crystals were obtained by complete evaporation of the eluted solution at room temperature. The yields were 0.125 g (47%) of green product and 0.052 g (19%) of the blue product.

2.5. Preparation of ccc-$Ru(papm)_2Cl_2$ (**4c**)

A 0.1-g (0.38 mmol) amount of $RuCl_3 \cdot 3H_2O$ and 0.15 g (0.82 mmol) of 2-(arylazo)pyrimidine in ethanol (30 cm^3) were refluxed under a dinitrogen atmosphere for 3 h. The mixture was cooled and the precipitate was filtered and washed with pet-spirit (60–80°C). The solid was then suspended in 60 cm^3 of toluene and refluxed for 2 h. The product was filtered hot and the solid was washed with pet-spirit (60–80°C). It was then dissolved in hot acetonitrile, and filtered and poured into three volumes of water. Then the mixture was allowed to settle overnight. The product was filtered and dried in vacuo over P_4O_{10}. It was then dissolved in a minimum volume of CH_2Cl_2 and chromatographed as earlier. The blue band was eluted using a 4:1 (v/v) benzene–acetonitrile mixture. Crystals were obtained by complete evaporation of the eluted solution at room temperature. The yield of ccc-$Ru(papm)_2Cl_2$ was 0.068 g (68%).

2.6. Isomer conversion, tcc (**4a**) (green)→ctc (**4b**) (blue)

Isomer conversion was carried out thermally. One representative case is detailed below. The green tcc-$Ru(papm)_2Cl_2$ (0.1 g, 0.19 mmol) was suspended in xylene (50 cm^3) and heated to reflux for 8 h (conversion was tested by TLC). The solution was filtered and the residue was washed with Et_2O. It was dissolved in a

minimum volume CH_2Cl_2 and subjected to chromatography as before. A very small green band was eluted slowly using 19:1 (v/v) benzene–acetonitrile along with a blue tail followed by a deep blue band that was eluted using 9:1 (v/v) benzene–acetonitrile. This blue solution was evaporated in air at room temperature and dark shining crystals were deposited. The yield was 0.082 g (82%). A similar conversion of (**4a**)→(**4c**) was carried out on boiling toluene and the yield was 78%.

2.7. X-ray crystallography

Crystals that were suitable for X-ray work were grown by slow diffusion of hexane into a dichloromethane solution at 298 K (crystal size: tcc-Ru(papm)$_2$Cl$_2$ (**4a**), 0.15×0.15×0.30 mm^3; ccc-Ru(papm)$_2$Cl$_2$ (**4c**), 0.14×0.17×0.19 mm^3). Data were collected on a Siemens SMART CCD diffractometer with graphite monochromatised Mo K_α radiation (λ=0.71073 Å) at 295 K. Data on the crystals and the collection parameters are listed in Table 1. The data were corrected for absorption effects by an empirical method using azimuthal scan data. Systematic absences led to the identification of space groups Pbca (orthorhombic crystal system) and $P2_1/C$ (monoclinic crystal system), respectively. Of the 17 278 (tcc) and 10 621 (ccc) collected reflections, 3065 and 3684 with $I>2\sigma(I)$ were used for structure solution, respectively. In both cases, the structures were solved by the conventional heavy-atom method and were refined by the full-matrix least-squares method on all F_0^2 data using the SHELXTL 5.03 package on Silicon Graphics Indigo-R4000 computers. In both cases, hydrogen atoms were included in calculated positions and refined with isotropic thermal parameters, which were ~1.2 [aromatic (H)] times the equivalent isotropic thermal parameters of their parent carbon atoms.

Table 1
Summarised crystallographic data for complexes **4a** and **4c**

Crystal parameters	**4a**	**4c**
Formula	$C_{20}H_{16}Cl_2N_8Ru$	$C_{20}H_{16}Cl_2N_8Ru$ 0.75(CH_2Cl_2)
M	540.38	604.07
Crystal system	Orthorhombic	Monoclinic
Space group	*Pbca*	$P2_1/c$
a/Å	13.0541(2)	14.9548(6)
b/Å	10.5734(2)	7.9177(3)
c/Å	31.1053(6)	21.6196(9)
β/°	90	91.520(1)
V/Å^3	4293.35(13)	2558.4(2)
λ/Å	0.71073	0.71073
ρ_{calcd}/mg m^{-3}	1.672	1.568
Z	8	4
T/K	298	298
μ(Mo K_α)/mm^{-1}	1.005	1.004
Refined parameters	281	308
R[a]	0.0291	0.0386
wR[b]	0.0897	0.1107
GOF[c]	0.826	1.034

[a] $R=\Sigma[F_0-F_c]/\Sigma F_0$.

[b] $wR=[\Sigma w(F_0^2-F_c^2)/\Sigma wF_0^4]^{1/2}$, $w=1/[\sigma^2(F_0^2)+(0.0473P)^2+14.3394P]$, $P=(F_0^2+2F_c^2)/3$.

[c] GOF is defined as $[w(F_0-F_c)/(n_0-n_v)]^{1/2}$, where n_0 and n_v denote the numbers of data and variables, respectively.

3. Results and discussion

3.1. Synthesis

2-(Arylazo)pyrimidines (aapm, **3**) were synthesised by condensing nitrosoaromatics (ArNO) with 2-aminopyrimidine in the presence of metallic sodium in dry benzene under refluxing conditions for 12 h. Purification was carried out by chromatography. The ligands are new and act as N,N′- bidentate chelating molecules. The donor centres are abbreviated as N(1)(pyrimidine), N and N(azo), N′, and the atom-numbering scheme is shown in the structure **3** (see Scheme 1). Ethanolic solutions of aapm react with $RuCl_3$ under reflux (over N_2) to afford the complex Ru(aapm)$_2$Cl$_2$ via spontaneous reductive chelation. Even when the ligand is used in excess of 2 mol equivalents, only Ru(aapm)$_2$Cl$_2$ is isolated from this reaction. The complexes were isolated in high yield from the reaction mixture. One isomer (green, isomer A) is sparingly soluble in ethanol and was isolated by filtration from the reaction mixture. The blue filtrate was evaporated and chromatographed on an alumina column. A blue isomer (isomer B) and a deep-blue isomer (isomer C) were eluted using 9:1 and 4:1 (v/v) benzene–acetonitrile mixtures, respectively. The elution trend may distinguish between the complexes based on polarity difference between them. Thus, isomer B is less polar than isomer C. The reaction of Ru(DMSO)$_4$Cl$_2$ and aapm in acetone yields isomer A as the major product.

The ligands have unsymmetric bidentate N,N′- donor centres. The pseudo-octahedral dichloro species, Ru(aapm)$_2$Cl$_2$, can, in principle, occur in five geometrically isomeric forms. Two (i and ii) of these have the $RuCl_2$ group in the *trans* geometry and the other three (iii–v) have the $RuCl_2$ group in the *cis* geometry. Considering the coordinating pairs in the order of Cl, Cl; N, N; N′, N′ where N represents N(pyrimidine) and N′ represents N(azo), the configurations of these five are *trans–cis–cis* [tcc, (i)], *trans–trans–trans* [ttt, (ii)], *cis–trans–cis* [ctc, (iii)], *cis–cis–cis* [ccc, (iv)] and *cis–cis–trans* [cct, (v)].

Isomer A (green complex) is almost quantitatively converted to isomer B on boiling in a suspension of xylene, while isomer C is produced when thermal transformation is carried out in a suspension of toluene. In the present work, three isomers were isolated that were green (**4a**–**6a**), blue (**4b**–**6b**) and deep blue (**4c**–**6c**) and these were characterised by spectral studies (vide infra) as tcc-, ctc- and ccc-Ru(aapm)$_2$Cl$_2$, respectively. Two of these three isomers, i.e., tcc-Ru(aapm)$_2$Cl$_2$ (**4a**) are ccc-

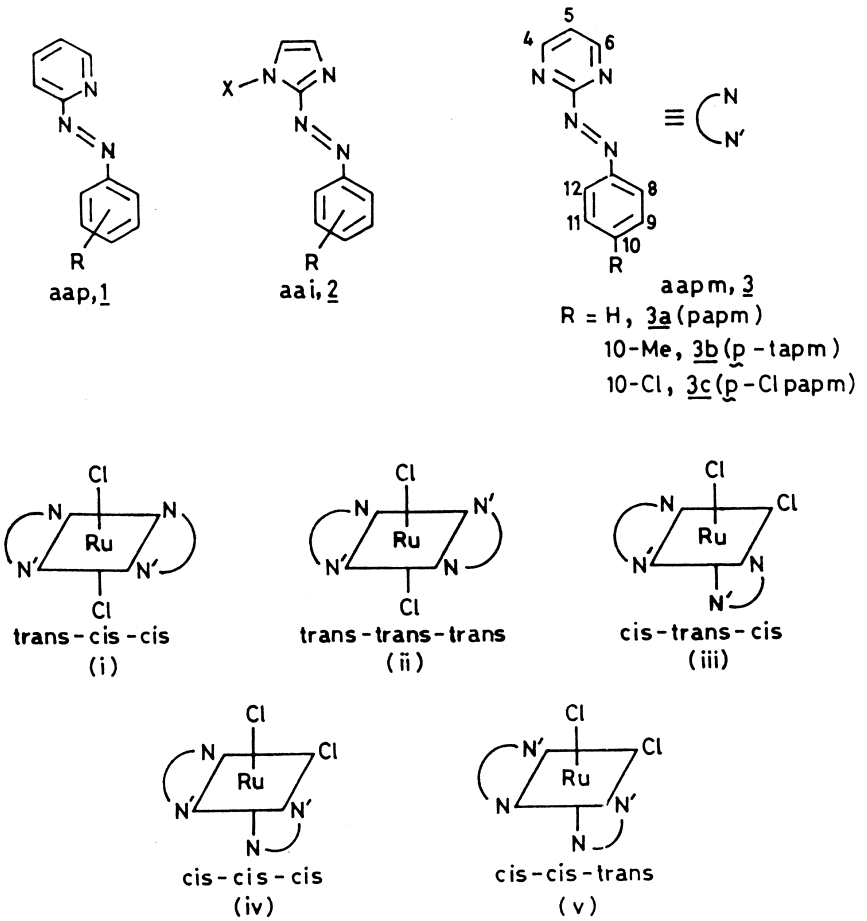

Scheme 1.

$Ru(aapm)_2Cl_2$ (**4c**), have been characterised by X-ray crystallographic methods. Crystallographic data for complexes **4a** and **4c** are shown in Table 1.

3.2. Molecular structures

The crystal structures of the green (**4a**; isomer A) and blue (**4c**; isomer C) isomers are shown in Figs. 1 and 2, and bond parameters are listed in Tables 2 and 3, respectively. The coordination around ruthenium is approximately octahedral. The atomic arrangement in **4a** involves sequentially two *trans*-chlorine, *cis*-pyrimidine-N(N) and *cis*-azo-N(N′) and corresponds to the *trans–cis–cis* configuration. Similarly, the arrangement in **4b** is *cis–cis–cis*.

*3.3. Green isomer, **4a***

The two atomic groups Ru, Cl(1), N(1), Cl(2), N(27) and Ru, Cl(1), N(21), Cl(2), N(7) separately constitute two excellent planes (mean deviation, 0.07 Å) and are orthogonal to the third molecular plane, Ru, N(1), N(7), N(27), N(21) (deviation, 0.08 Å). The Ru atom is shifted by 0.04 Å from the centre of gravity of the third plane

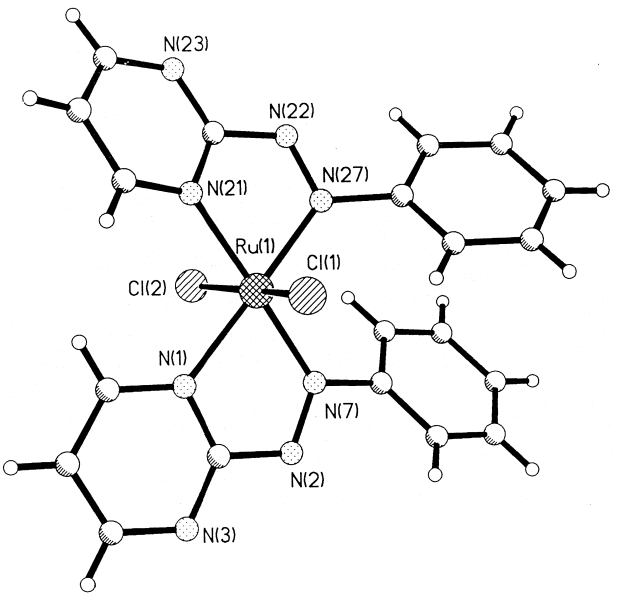

Fig. 1. Crystal structure and atom-labelling scheme for tcc-$Ru(papm)_2Cl_2$ (**4a**).

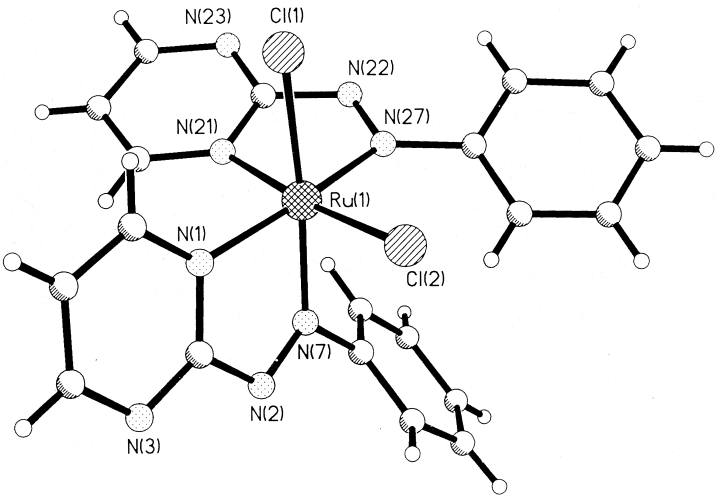

Fig. 2. Crystal structure and atom-labelling scheme for ccc-Ru(papm)$_2$Cl$_2$ (**4c**).

Table 2
Selected bond distances (Å) and angles (°) for complex **4a**, along with their estimated standard deviations

Distances			
Ru–N(1)	2.093(3)	Ru–N(21)	2.072(3)
Ru–N(7)	2.000(3)	Ru–N(27)	2.005(3)
Ru–Cl(1)	2.363(1)	Ru–Cl(2)	2.401(1)
N(2)–N(7)	1.299(5)	N(22)–N(27)	1.306(5)
Angles			
N(1)–Ru–N(7)	75.64(13)	N(21)–Ru–N(7)	176.75(12)
N(1)–Ru–Cl(1)	87.75(9)	N(21)–Ru–N(27)	75.78(12)
N(1)–Ru–Cl(2)	86.03(9)	N(21)–Ru–Cl(1)	88.35(9)
Ru–N(7)–N(2)	121.2(3)	N(21)–Ru–Cl(2)	85.40(9)
N(7)–Ru–N(27)	105.53(13)	Cl(1)–Ru–Cl(2)	169.99(4)
N(7)–Ru–Cl(1)	94.49(9)	N(27)–Ru–Cl(1)	94.19(9)
N(7)–Ru–Cl(2)	91.57(9)	N(27)–Ru–Cl(2)	91.86(9)
N(1)–Ru–N(27)	177.63(12)	Ru–N(27)–N(22)	117.6(2)
N(1)–Ru–N(21)	102.95(12)		

Table 3
Selected bond distances (Å) and angles (°) for complex **4c**, along with their estimated standard deviations

Distances			
Ru–N(1)	2.047(3)	Ru–Cl(1)	2.394(1)
Ru–N(21)	2.027(3)	Ru–Cl(2)	2.401(1)
Ru–N(7)	1.971(3)	N(2)–N(7)	1.286(5)
Ru–N(27)	2.014(3)	N(22)–N(27)	1.295(5)
Angles			
N(1)–Ru–N(7)	76.50(14)	N(1)–Ru–N(21)	96.27(14)
N(1)–Ru–Cl(1)	94.62(11)	N(21)–Ru–N(27)	77.01(13)
N(1)–Ru–Cl(2)	84.91(11)	N(21)–Ru–Cl(1)	84.06(10)
N(7)–Ru–Cl(1)	170.58(10)	N(21)–Ru–Cl(2)	172.75(9)
N(7)–Ru–Cl(2)	87.38(11)	N(27)–Ru–Cl(1)	87.02(9)
Ru–N(7)–N(2)	121.00(3)	N(27)–Ru–Cl(2)	102.04(10)
N(7)–Ru–N(27)	102.18(13)	Ru–N(27)–N(22)	117.6(3)
N(7)–Ru–N(21)	99.85(14)	N(1)–Ru–N(27)	172.91(14)
Cl(1)–Ru–Cl(2)	88.72(4)		

towards Cl(1). The N(1)–Ru–N(27) angle is 177.63(12)°; this deviation originates undoubtedly from the acute [(75.78(12)°] chelate bite angle [31]. The chelate ring, Ru, N(1), C(2), N(2), N(7), is planar (deviation, 0.04 Å) while Ru, N(21), C(21), C(22), N(12), N(27) is distorted to a somewhat greater extent (deviation, 0.13 Å) and the dihedral angle is 169°. The *trans*-chlorine angle is 169.99(4)°. The structure of the molecule is shown in Fig. 1 and the bond parameters are listed in Table 2.

The Ru–N′[N(azo): N(7) or N(27)] bond distance (average, 2.00 Å) is shorter than the Ru–N[N(pyrimidine): N(1) or N(21)] (average, 2.08 Å) bond distance by ~0.08 Å. The shortening may be due to greater π-backbonding, d(Ru)→π*(azo). The N–N distance is not available for this free ligand; however, the data available in some free azo ligands suggest that it is ca. 1.25 Å [20,21]. In the complex, the N–N distance is 1.299(5) Å. The coordination can lead to a decrease in the N–N bond order due to both the σ-donor and π-acceptor character of the ligands, with the latter character having a more pronounced effect, which may be the reason for elongation (supported by spectral data). The pendant phenylazo rings are planar and are inclined at angles of 41 and 35° relative to the chelated azoimine fragment, suggesting stereochemically nonequivalent C–H functions. Two *cis*-phenylazo planes are semiparallel and are inclined at an angle of 22°. The minimum distance between the centroid of phenyl rings is 3.716 Å.

3.4. Blue isomer, ***4c***

The atomic groups Ru, Cl(2), N(27), N(21) (mean deviation, 0.08 Å) and Ru, Cl(1), N(27), N(7), N(1) (mean deviation, 0.09 Å) constitute two almost orthogonal (dihedral angle, 88°) planes. The third plane, Ru, Cl(1), N(21), N(7), Cl(2) (mean deviation, 0.08 Å), is less orthogonal (dihedral angles, 98.7° and 82.6°, respectively,

with earlier planes). The structure is shown in Fig. 2 and the bond parameters are listed in Table 3. The *trans* angles around the ruthenium centre in the planes range from 170.58 to 172.91°, indicating distortion from rectilinear geometry. The chelate angles extended by azopyrimidine are 76.5(1)° and 77.0(1)° and are considerably deviated from the ideal octahedral geometry. As a consequence of the constraint of the bite angle, the ligands are bent back from the coordinated chlorides. The chelate rings, Ru, N(1), C(2), N(2), N(7) (mean deviation, 0.05 Å) and Ru, N(21), C(22), N(22), N(27) (mean deviation, 0.08 Å), are planar and the dihedral angle is 73°. It is noticeable that most of the distortions away from octahedral positions arising out of the larger angular distortions are associated with the azo nitrogens rather than the pyrimidine nitrogens [N(7)–Ru–N(27), 102.18(13)°; N(1)–Ru–N(21), 96.27(14)°]. The *cis*-chloro angle of 88.72 (4)° is very nearly the ideal octahedral angle and is comparable to reported values [31]. The chelate rings are planar (mean deviation, 0.06 Å) and are inclined at an angle of 73°. The N–N distance is shorter than that in its green counterpart. The Ru–N(pyrimidine) distances (2.047, 2.027 Å) are longer than those of Ru–N(azo) (1.971, 2.014 Å) and this is an indication of an M–L π-interaction that is localised in the M–azo fragment. The Ru–Cl distance is comparable with the reported values [20,21,31]. The pendant phenyl rings are planar and are inclined at an acute angle with the respective chelate rings. The dihedral angles between the chelate ring and the corresponding phenyl ring are 51.6 and 23.2°.

3.5. Spectra

The green complexes exhibit a single, intense, sharp stretching frequency in the range 325–300 cm^{-1} that can be assigned to ν(Ru–Cl) and a band in the region 235–220 cm^{-1} that is due to ν(Ru–N)(pyrimidine). The blue complexes exhibit two Ru–Cl stretches in the ranges 330–300 and 280–250 cm^{-1}, supporting the *cis*-$RuCl_2$ configuration. All of the complexes exhibit intense bands at 1580 and 1400 cm^{-1}, corresponding to C=N and N=N stretchings, respectively. Heterocyclic ring deformations are observed at the usual positions [38–44], i.e., 1540, 1480, 1290, 1190, 1164, 1090, 1010, 965 cm^{-1} etc. The ligands (**3**) exhibit a sharp band at 1420–1440 cm^{-1}, corresponding to N=N, and C=N appears as a single sharp, intense stretch at around 1600 cm^{-1}. In the complexes, ν(N=N) is red shifted by 25–30 cm^{-1}, which is a good indication of N-coordination.

UV–visible spectral studies of the complexes reveal absorptions within the range 200–900 nm (Table 4). The free ligands exhibit transitions at 360–370 nm (ϵ~20,000) and 430–450 nm (ϵ~500), which are due to intraligand charge transfer transitions, $\pi\rightarrow\pi^*$ and $n\rightarrow\pi^*$, respectively, centred primarily on the azo group. Thus, the transitions in the complexes at around 400 nm are probably of ligand origin and were not considered further. The green complexes (**4a**–**6a**) show an intense (ϵ~10^4) band in the region 623±5 nm, along with a weak shoulder at around 726±4 nm (ϵ~10^3), and are assigned to the t_2(Ru)→ π*(L) (MLCT) transition, where the π* orbital has a large azo character [31]. Blue complexes exist in two isomeric forms and both exhibit highly intense (ϵ~10^4) MLCT transitions at higher energies compared to the green complex: the main band is observed in the range 580–595 nm while a weak shoulder (ϵ~10^3) appears in the range 760–830 nm. The energy of the MLCT transition is symmetry-dependent [63–65]. The X-ray structural study (vide supra) confirms that isomer A belongs to tcc-Ru(aapm)$_2$Cl$_2$ (C_2 symmetry) and that isomer C belongs to ccc-Ru(aapm)$_2$Cl$_2$ (C_1 symmetry) configurations, respectively. It is evident from IR data that isomer B has a *cis*-$RuCl_2$ configuration, thus, it may be of either the cct or ctc type (both belong to C2 symmetry). The less symmetric ccc isomer should exhibit a stronger interaction compared to the other isomers. On comparing our results with results reported for similar systems [6–19,31], ruthenium(II)–arylazopyridine complexes, we may conclude that isomer B is ctc-Ru(aapm)$_2$Cl$_2$. However, we have no structural evidence to support this. The ccc-Ru(aapm)$_2$Cl$_2$ isomer exhibits a transition at a higher energy (~10 nm) than that of the ctc isomer. The more intense band at the higher energy is believed to be the spin-allowed singlet–singlet transition and the weaker band at lower energy could be the corresponding singlet–triplet transition mode, which is allowed by the strong spin–orbit coupling in ruthenium [31].

The ^{1}H NMR spectra of the ligands and complexes were compared to determine the binding mode and stereochemistry of the complexes. The proton-numbering pattern is shown in aapm (**3**) and are assigned on the basis of spin–spin interaction and changes therein on substitution. The spectrum of the ligand is cleanly divided into two parts (Table 5). The downfield portion is due to the pyrimidine protons (4-6-H) [38–44] and the upfield signals refer to azoaryl protons (8-12-H). Aryl protons are affected by substitution; 9- and 11-H are mostly perturbed due to changes in the electronic properties of the substituents in the 10-position. The proton's movement is corroborated with the electromeric effect of the group. In the complexes, 4- and 6-H are downfield-shifted whereas 5-H either remains unshifted or moves upfield relative to the free ligand values. The Ar-Me signal has been particularly useful in determining isomer configuration. The tcc- and ctc-Ru(*p*-tapm)$_2$Cl$_2$ have C_2-symmetry and a single Ar-Me signal while ccc-Ru(*p*-tapm)$_2$Cl$_2$ is C_1-symmetric and is expected to exhibit two -Me signals of equal intensities (Fig. 3). This is indeed observed. The aryl protons 9,11-(9′,11′-)H in Ru(aapm)$_2$Cl$_2$ resonate symmetrically at a

Table 4
Analytical[a], UV–Vis spectral[b] and voltammetric data[c–e]

Compound	Analysis (%)			λ_{max}, nm ($10^{-3}\epsilon$, M^{-1} cm^{-1})	Ru(III)/Ru(II) $E^{M}_{1/2}$(ΔE, mV)	Ligand reduction $-E^{L}_{1/2}$, V (ΔE_p, mV)
	C	H	N			
3a papm	65.18 (65.21)	4.30 (4.35)	30.39 (30.43)	431(0.42), 355(19.85), 225(7.46)		1.14(130), 1.42(170)
3b *p*-tapm	66.68 (66.66)	5.00 (5.05)	28.26 (28.28)	446(0.51), 360(26.72), 224(8.98)		1.19(140), 1.37(180)
3c *p*-Clpapm	54.90 (54.92)	3.18 (3.20)	25.65 (25.63)	447(0.26), 370(12.20), 224(3.85)		1.09(150), 1.30(180)
4a *tcc*-Ru(papm)$_2$Cl$_2$	44.46 (44.44)	2.94 (2.96)	20.71 (20.74)	723(5.44), 28(10.80), 433(11.13), 251(17.69)	1.08(77)	0.48(120), 0.69(170), 1.21[e]
4b *ctc*-Ru(papm)$_2$Cl$_2$	44.40 (44.44)	2.97 (2.96)	20.73 (20.74)	830(0.82)[f], 592(7.71), 403(8.73), 372(13.63), 251(14.34)	1.24(80)	0.40(87), 0.61(104), 1.32[e]
4c *ccc*-Ru(papm)$_2$Cl$_2$	44.47 (44.44)	3.00 (2.96)	20.73 (20.74)	809(0.82)[f], 575(7.70), 416(8.96), 372(15.43), 252(17.49)	1.31(63)	0.41(76), 0.81(80), 1.38[e]
5a *tcc*-Ru(*p*-tapm)$_2$Cl$_2$	46.50 (46.48)	3.51 (3.52)	19.70 (19.72)	724(4.81), 625(11.46), 448(12.04), 372(15.69), 257(17.75)	1.00(85)	0.54(80), 1.06(67), 1.43[e]
5b *ctc*-Ru(*p*-tapm)$_2$Cl$_2$	46.47 (46.48)	3.53 (3.52)	19.74 (19.72)	838(0.79)[f], 595(8.05), 425(11.35) 375(16.82), 250(18.20)	1.18(80)	0.53(90), 0.78(120), 1.31[e]
5c *ccc*-Ru(*p*-tapm)$_2$Cl$_2$	46.50 (46.48)	3.51 (3.52)	19.71 (19.72)	820(1.08)[f], 587(9.47), 437(13.15), 397(21.62), 252(20.13)	1.21(88)	0.46(90), 1.10(66), 1.42[e]
6a *tcc*-Ru(*p*-Clpapm)$_2$Cl$_2$	39.41 (39.40)	2.32 (2.30)	18.41 (18.39)	732(4.84), 623(10.51), 441(12.10), 391(15.65), 251(22.49)	1.17(100)	0.41(100), 0.64(120), 1.14[e]
6b *ctc*-Ru(*p*-Clpapm)$_2$Cl$_2$	39.42 (39.40)	2.28 (2.30)	18.38 (18.39)	842(0.86)[f], 588(8.33), 406(12.90) 368(18.67), 252(17.32)	1.34(102)	0.35(90), 0.54(110), 1.20[e]
6c *ccc*-Ru(*p*-Clpapm)$_2$Cl$_2$	39.39 (39.40)	2.29 (2.30)	18.41 (18.39)	760(1.23)[f], 580(6.17), 428(8.34), 388(12.22), 254(15.14)	1.40(81)	0.34(88), 0.51(90) 1.25[e]

[a] Calculated values are given in parentheses.
[b] In CH_3CN.
[c] Meaning and units of the symbols are the same as in text.
[d] Solvent in CH_3CN. Supporting electrolyte, TBAP (0.01 M); solute concentration, 10^{-3} M; scan rate, 0.05 V s^{-1}.
[e] Cathodic peak potential E_{pc}, V.
[f] Shoulder.

Table 5
^{1}H NMR data for the compounds[a] [δ/ppm, (J/Hz)]

Compound	4-H[b]	5-H[c]	6-H[b]	8-H[b]	9-H	10-H	11-H	12-H[b]	Ar-Me
3a	8.24 (7.0)	8.10[d]	8.24 (7.0)	7.83 (9.0)	7.45[c] (8.0)	7.58[d]	7.45[c] (8.0)	7.83 (9.0)	
3b	8.20 (7.4)	8.10[d]	8.20 (7.4)	7.80 (9.0)	7.31 (8.0)		7.31 (8.0)	7.80 (9.0)	2.43
3c	8.30 (7.8)	8.14[d]	8.30 (7.8)	7.88 (8.0)	7.54 (8.0)		7.54 (8.0)	7.88 (8.0)	
4a	8.92 (7.5)	7.78 (8.0)	9.15 (9.0)	7.59 (7.5)	7.00 (7.8)	7.24[d]	7.00 (7.8)	7.69 (7.5)	
4b	9.06 (9.0)	7.85 (7.5)	9.88 (9.0)	7.66 (7.5)	7.18 (7.5)	7.39[d]	7.15 (7.5)	7.82 (7.5)	
4c	9.17 (9.0)	7.88 (8.4)	9.95 (9.0)	7.71 (7.5)	7.23 (8.0)	7.41[d]	7.23 (8.0)	9.98 (7.5)	
5a	8.85 (8.4)	7.69 (8.4)	9.02 (9.0)	7.52 (7.5)	6.65 (7.5)		6.65 (7.5)	7.61 (7.5)	2.48
5b	8.97 (8.1)	7.75 (8.1)	9.75 (9.0)	7.60 (8.4)	6.82 (8.4)		6.82 (8.4)	7.77 (8.4)	2.53
5c	9.00 (8.4)	7.81 (7.5)	9.83 (8.4)	7.69 (7.5)	6.91 (7.5)		6.91 (7.5)	7.92 (7.5)	2.65, 2.52
6a	8.92 (7.8)	7.77 (8.4)	9.22 (9.0)	7.58 (7.8)	7.06 (7.5)		7.66 (7.5)	7.68 (7.8)	
6b	9.08 (8.4)	7.88 (8.4)	9.90 (8.4)	7.68 (7.8)	7.21 (7.8)		7.21 (7.8)	7.84 (7.8)	
6c	9.19 (9.0)	7.91 (7.8)	9.98 (9.0)	7.74 (7.5)	7.25 (7.8)		7.25 (7.8)	7.96 (7.5)	

[a] Solvent in $CDCl_3$.
[b] Doublet.
[c] Triplet.
[d] Multiplet.

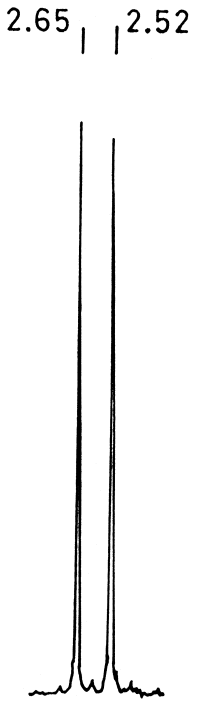

Fig. 3. Ar-Me signal of ccc-Ru(p-tapm)$_2$Cl$_2$ (**5c**) in $CDCl_3$ showing inequivalence character.

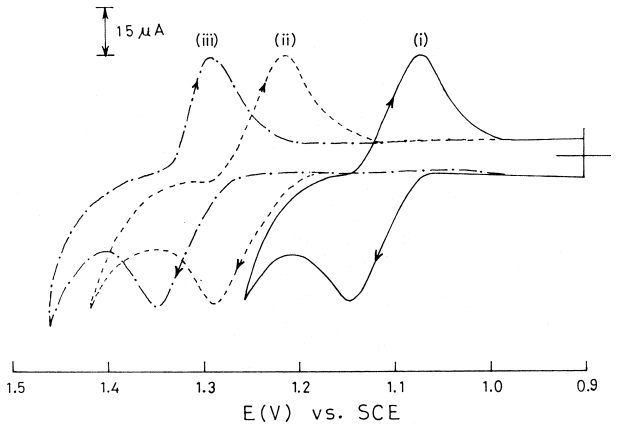

Fig. 4. Cyclic voltammogram in MeCN (0.1 M TBAP) at a Pt-bead working electrode. The solute concentration and scan rate are 10^{-3} M and 50 mV s^{-1}, respectively. (i) tcc-Ru(papm)$_2$Cl$_2$ (**4a**) (green) (———); (ii) ctc-Ru(papm)$_2$Cl$_2$ (**4b**) (blue) (- - -) and (iii) ccc-Ru(papm)$_2$Cl$_2$ (**4c**) (deep blue) (– · –).

single position, while 8-(8′-)H and 12-(12′-)H resonate asymmetrically, which is indicative of a magnetically different environment. The 12-(12′-)H is stereochemically nearer than 8-(8′-)H to the metal centre. In blue complexes (ctc- and ccc-isomers), the steric effect induces more distortion and is reflected from greater separation in signal resonance of 12-(12′-)H and 8-(8′-)H. The separation follows the order ccc>ctc>tcc and average values are 75, 48 and 30 Hz, respectively.

3.6. Electrochemistry and correlation with electronic spectra

The electrochemical behaviour of the complexes in MeCN was examined by cyclic voltammetry. The voltammogram displayed metal oxidations on the positive side and the ligand reductions on the negative with respect to SCE. The results are given in Table 4 and a representative voltammogram is shown in Fig. 4.

In the potential range +0.5 to +2.0 V at a scan rate 50 mV s^{-1} in acetonitrile, one reversible-to-quasireversible (peak-to-peak separation ΔE_p, 60–100 mV) oxidative response is observed corresponding to the couple (1) at the platinum disc electrode surface.

$$Ru(aapm)_2Cl_2^+ + e^- \rightleftharpoons Ru(aapm)_2Cl_2 \quad (1)$$

The data (Table 4) reveal that the blue complexes (ctc and ccc) exhibit higher potentials by 0.1–0.2 V than the green complexes. In the blue isomers, the two azo functions are *cis* oriented and a back-bonding interaction may occur with two different dπ-orbitals, which may lead to an increase in the effective charge on the ruthenium centre. The ccc isomer shows a higher Ru(III)/Ru(II) couple (0.07–0.1 V) than that of the ctc isomer. This may be due to reduced symmetry (C_1-symmetry) in ccc isomer relative to ctc (C_2-symmetry) isomer, which may lead to a better Ru–L interaction. This is also supported by electronic spectral data.

The Ru(III)/Ru(II) redox potential of the present examples is the highest amongst the known complexes of the azoimine system. The higher π-acidity of azoimine compared to bipyridine is reflected by the higher potential of the former [20,21]. Ru(aai)$_2$Cl$_2$ shows the couple in the range 0.6–0.9 V; while arylazopyridine complexes, Ru(aap)$_2$Cl$_2$, are exhibited the same at 0.9–1.2 V. The present complexes Ru(aapm)$_2$Cl$_2$ exhibit the highest potential (1.1–1.4 V) in this family. This is in accord with the π-acidity order [36,37] of the ligands: bipyridine< azoimidazole< azopyridine< azopyrimidine. The azopyrimidine ligands thus stabilise (with respect to oxidation) ruthenium (II) better than the azopyridines.

In the potential range 0.0–1.8 V, reductive responses are observed under similar conditions using a glassy carbon working electrode. The reduced species appears to be less stable and, on scan reversal, multiple anodic responses are observed. The reduction responses were compared with the results for free ligands. The free ligand displays two quasireversible one-electron cyclic voltammetric responses with peak-to-peak separation in the range 130–180 mV, corresponding to the couples in Eq. (2):

$$aapm \overset{e^-}{\rightleftharpoons} aapm^- \overset{e^-}{\rightleftharpoons} aapm^{2-} \quad (2)$$

The formal potentials of these couples are −1.2 and −1.4 V, respectively, which are less than that of the

azopyridine analogues by 0.1–0.2 V. In ruthenium(II) complexes, as expected, the reduction potential displays a substitutional positive shift from the corresponding free ligand values.

The difference in two successive redox responses at positive and negative to SCE [$\Delta E^0 = E^0_M(2) - E^0_L(3)$] may be correlated with MLCT transitions. The electronic excitation may be considered as an intramolecular redox process and the energy, ν_{CT}, of the lowest MLCT transition is expected to be linearly related to ΔE^0. The least squares plot of ν_{CT} (in eV) against ΔE^0 (V) corresponds to Eq. (3), with coefficient of correlation squared is 0.942. A similar correlation has been observed [1–5,31] for bpy, arylazopyridine and arylazoimidazole complexes.

$$\nu_{CT} = 0.962\ \Delta E^0 + 0.491 \quad (3)$$

Supplementary data

Supplementary data are available from the Cambridge Crystallographic Data Centre, 12 Union Road, Cambridge CB2 1EZ, UK, on request, quoting the deposition numbers CCDC 116289 (for **4a**) and CCDC 116290 (for **4c**). Atomic coordinates (SHELXTL 5.03 program system; Siemens Analytical X-ray instruments, Madison, WI, 1995) and isotopic thermal parameters are listed in Tables SI–SVIII (in supplementary data).

Acknowledgements

Financial assistance from the University Grants Commission, New Delhi, is gratefully acknowledged. T.K.M. is thankful to the Council of Scientific and Industrial Research, New Delhi, for a fellowship. We thank Prof. R. Venkataswaran, Indian Association for the Cultivation of Science, Calcutta, for recording the NMR spectra.

References

[1] B.K. Ghosh, A. Chakravorty, Coord. Chem. Rev. 95 (1989) 239.
[2] B.K. Santra, G.A. Thakur, P. Ghosh, K.A. Pramanik, G.K. Lahiri, Inorg. Chem. 35 (1996) 3050.
[3] J. Chakravorty, S. Bhattacharya, Trans. Metal Chem. 20 (1995) 138.
[4] T.K. Malik, P.K. Das, B.K. Roy, B.K. Ghosh, J. Chem. Res. (S) (1993) 374.
[5] M. Kakoti, S. Chaudhury, A.K. Deb, S. Goswami, Polyhedron 12 (1993) 783.
[6] R.A. Krause, K. Krause, Inorg. Chem. 23 (1984) 2195.
[7] R.A. Krause, K. Krause, Inorg. Chem. 21 (1982) 1714.
[8] R.A. Krause, K. Krause, Inorg. Chem. 19 (1980) 2600.
[9] B. Teil, Z. Naturoforsch 50 (1995) 15.
[10] N. Bag, G.K. Lahiri, A. Chakravorty, Inorg. Chem. 31 (1992) 40.
[11] G.K. Lahiri, S. Bhattacharya, S. Goswami, A. Chakravorty, J. Chem. Soc., Dalton Trans. (1990) 561.
[12] G.K. Lahiri, S. Goswami, L.R. Falvello, A. Chakravorty, Inorg. Chem. 26 (1987) 3365.
[13] A.K. Mahapatra, B.K. Ghosh, S. Goswami, A. Chakravorty, J. Indian Chem. Soc. 63 (1986) 101.
[14] P. Ghosh, A. Chakravorty, J. Chem. Soc., Dalton Trans. (1985) 361.
[15] A. Seal, S. Ray, Acta Crystallogr., Sect. C: Struct. Commun. 40 (1984) 929.
[16] S. Goswami, R.N. Mukherjee, A. Chakravorty, Inorg. Chem. 22 (1983) 2825.
[17] S. Goswami, A.R. Chakravorty, A. Chakravorty, Inorg. Chem. 22 (1983) 602.
[18] S. Goswami, A.R. Chakravorty, A. Chakravorty, J. Chem. Soc., Chem. Commun. (1982) 1288.
[19] S. Goswami, A.R. Chakravorty, A. Chakravorty, Inorg. Chem. 20 (1981) 2246.
[20] B.K. Ghosh, S. Goswami, A. Chakravorty, Inorg. Chem. 22 (1983) 3358.
[21] B.K. Ghosh, A. Mukhopadhyay, S. Goswami, S. Ray, A. Chakravorty, Inorg. Chem. 23 (1984) 4633.
[22] D. Datta, A. Chakravorty, Inorg. Chem. 22 (1988) 1085.
[23] P. Chattopadhyay, B.K. Dolui, C. Sinha, Indian J. Chem. 36A (1997) 489.
[24] D. Das, M.K. Nayak, C. Sinha, Trans. Metal Chem. 22 (1997) 172.
[25] D. Das, C. Sinha, Indian J. Chem. 37A (1998) 531.
[26] D. Das, C. Sinha, Trans. Metal Chem. 23 (1998) 517.
[27] T.K. Misra, D. Das, C. Sinha, Polyhedron 16 (1997) 4163.
[28] D. Das, T.K. Misra, C. Sinha, Trans. Metal Chem. 23 (1998) 73.
[29] T.K. Misra, C. Sinha, Indian J. Chem. 38A (1999) 82.
[30] T.K. Misra, D. Das, C. Sinha, J. Indian Chem. Soc. 76 (1999) 125.
[31] T.K. Misra, D. Das, C. Sinha, P. Ghosh, C.K. Pal, Inorg. Chem. 37 (1998) 1672.
[32] P. Chattopadhyay, C. Sinha, D.K. Pal, Fresenius J. Anal. Chem. 357 (1997) 368.
[33] R. Argazzi, C.A. Bignozzi, T.A. Heimer, G.J. Meyer, Inorg. Chem. 36 (1997) 2.
[34] C.Y. Hung, T.L. Wang, Y. Jang, W.Y. Kim, R.H. Schmehl, R.P. Thummel, Inorg. Chem. 35 (1996) 5953.
[35] J.A. Real, M.C. Munoz, E. Andres, T. Granier, B. Gallios, Inorg. Chem. 33 (1994) 3587.
[36] E.C. Constable, Coord. Chem. Rev. 93 (1989) 205.
[37] T. Yamamoto, Z. Zhou, T. Kanbara, M. Shimura, K. Kizu, T. Maruyama, Y. Nakamura, T. Fukuda, B. Lee, N. Ooba, S. Tomaru, T. Kurihara, T. Kaino, K. Kubota, S. Sasaki, J. Am. Chem. Soc. 118 (1996) 10389.
[38] F. Zamora, M. Kunsman, M. Sabat, B. Lippart, Inorg. Chem. 36 (1997) 1583.
[39] M. Louloudi, Y. Deligiannakis, J.-P. Tuchagues, B. Donnadien, N. Nadjiliadis, Inorg. Chem. 36 (1997) 6335.
[40] F. Jolibois, J. Cadet, A. Grand, R. Subra, N. Raga, V. Barone, J. Am. Chem. Soc. 120 (1998) 1864.
[41] A.R. Katritzky, C.W. Pees, A.J. Boulton, Mckillop, Comp. Heterocyclic Chem. 3 (1984) 57.
[42] R.J. Guajardo, J.D. Tan, P.K. Mascharak, Inorg. Chem. 33 (1994) 2838.
[43] E. Colacio, J. Ruiz, J.M. Moreno, R. Kivekas, M.R. Sundberg, J.M. Dominguez-Vera, J.P. Laurent, J. Chem. Soc., Dalton Trans. (1993) 157.
[44] P.D. Cookson, R.T. Tiekimk, J. Chem. Soc., Dalton Trans. (1993) 259.
[45] F. Lloret, G. De Munno, M. Julve, J. Cano, R. Ruiz, A. Caneschi, Angew. Chem. Int. Ed. Engl. 37 (1998) 135.
[46] J.H. Groen, P.W.N.M. Van Leeuwen, K. Vrieze, J. Chem. Soc., Dalton Trans. (1998) 113.
[47] R. Cortes, M.K. Urtiaga, L. Lezama, J.L. Pizarro, M.I. Arriortua, T. Rojo, Inorg. Chem. 36 (1997) 5016.
[48] G. De Munno, G. Viau, M. Juleve, F. Llret, J. Faus, Inorg. Chim. Acta 257 (1997) 12.
[49] S.W. Keller, Angew. Chem. Int. Ed. (Engl.) 36 (1997) 247.
[50] G. De Munno, M. Juleve, J.A. Real, Inorg. Chim. Acta 255 (1997) 185.

[51] G. De Munno, W. Ventura, G. Vian, F. Lloret, J. Faus, M. Julve, Inorg. Chem. 37 (1998) 1458.
[52] B. Neuman, T. Hegmann, R. Wolf, C. Tschierske, Chem. Commun. (1998) 105.
[53] N. Arwaroli, F. Barigelletli, G. Calogeso, L. Flamigni, C.M. White, M.D. Ward, Chem. Commun. (1997) 2181.
[54] F. Baumann, W. Kaim, Inorg. Chem. 37 (1998) 658.
[55] B.T. Patterson, F. Keene, Inorg. Chem. 37 (1998) 645.
[56] Y. Chen, F.-T. Lin, R.E. Shepherd, Inorg. Chim. Acta 268 (1998) 287.
[57] Y. Jashng, R.P. Thummel, S.G. Bolt, Inorg. Chem. 36 (1997) 3139.
[58] F. Casalboni, Q.G. Mulazzami, C.D. Clark, M.Z. Hoffman, P.L. Orizondo, M.W. Perkovic, D.P. Rillema, Inorg. Chem. 36 (1997) 2252.
[59] V.M.R. Bailley, K.J.L. Galang, P.F. Doan, M.J. Clarke, Inorg. Chem. 36 (1997) 1873.
[60] G. Tresoldi, S. Lo Sclaro, P. Piraino, P. Zanello, J. Chem. Soc., Dalton Trans. (1996) 885.
[61] J.W.M. van Outersterp, F. Hartl, D.J. Stufkeng, Inorg. Chem. 33 (1994) 2711.
[62] B.T. Khan, S.V. Kumari, K.M. Mohan, Indian J. Chem. 31A (1992) 28.
[63] T.K. Misra, D. Das, C. Sinha, Indian J. Chem. 38A (1999) 416.
[64] A.B.P. Lever, Inorganic Electronic Spectroscopy, Elsevier, Amsterdam, 1968.
[65] A.B.P. Lever, Coord. Chem. Rev. 43 (1982) 63.